ORIGINAL RESEARCH **Open access**

Techno-Economic Evaluation of Electrochemical and Hydrogen-Based Energy Storage for Renewable Energy Systems

Chinedu Okafor[1*], Amina Bello[1], Ibrahim Musa[2]

Abstract

Energy storage serves as a practical solution to mitigate the volatility inherent in renewable power generation systems, including wind and solar, which are anticipated to be essential components of a sustainable, low-carbon future. Financial viability and carbon footprints represent critical metrics that require careful consideration when assessing the practicality of energy storage technologies (ESTs). This research investigates two viable pathways for massive-scale renewable energy storage—electrochemical energy storage (EES) and hydrogen energy storage (HES)—through a detailed technical evaluation of these ESTs. Comprehensive lifecycle assessments covering the levelized cost of storage (LCOS), carbon emission profiles, and uncertainty analyses for both EES and HES are executed, accounting for all essential stages within their operational pathways. To minimize assessment inaccuracies, the Monte Carlo simulation technique is employed to generate extensive datasets, thereby facilitating robust estimations of the economic performance and carbon output of ESTs derived from empirical data. Findings indicate that lithium-ion (Li-ion) batteries exhibit the most favorable LCOS and lowest carbon footprint among EES battery options, registering at 0.314 US kWh-1 and 72.76 gCO2e kWh-1, respectively. Various HES configurations—comprising distinct combinations of generation, distribution, and refueling methodologies—demonstrate considerable economic variance; the optimal LCOS and carbon emission values of 0.227 US kWh-1 and 61.63 gCO2e kWh-1 are attained via a pathway utilizing an alkaline electrolyzer (AE) for production, pipeline networks for delivery, and the associated refueling infrastructure. The conclusions drawn from this investigation imply that HES and EES exhibit comparable economic and environmental performance, indicating that both technologies warrant consideration for grid-scale renewable energy storage to meet prospective decarbonization targets.

Keywords Large-scale renewable energy storage, Techno-economic analysis, Carbon emissions, Electrochemical energy storage, Hydrogen energy storage

*Correspondence:
Chinedu Okafor
chinedu.okafor@gmail.com
[1] Department of AI for Distributed Energy Systems and Smart Microgrids, Faculty of Engineering, University of Lagos, Lagos, Nigeria
[2] Department of Intelligent Energy Analytics and Machine Learning, Faculty of Engineering, University of Ibadan, Ibadan, Nigeria

Introduction

The links between carbon emissions and global climate shifts and the greenhouse effect are increasingly evident [1-3]. Mitigating carbon output within the energy industry has emerged as a universal goal for securing sustainable development [3-5]. Progressively elevating the share of renewable energy to supersede conventional fossil fuels as the dominant power source is a vital strategy for driving the decarbonization transition; however, the severe fluctuations and unpredictability of renewable electricity generation present major hurdles [6-8]. Integrating energy storage infrastructure

This is an open access article distributed under the terms of the Creative Commons Attribution-NonCommercial-ShareAlike 4.0 International License (CC BY-NC-SA 4.0), which permits non-commercial use, distribution, reproduction, and adaptation in any medium or format, provided that appropriate credit is given to the original author(s) and source, a link to the license is provided, and any changes made are indicated. Adapted material must be distributed under the same license.

© 2025 The Author(s). | Published by Institute of Smart Energy Systems Press

with renewable generation networks offers a viable resolution to this challenge [9-11]. Storage systems contribute significantly to peak load shaving, thereby bolstering the reliability and security of power delivery in energy portfolios characterized by high renewable penetration [11, 12]. Consequently, scaling up energy storage capacities is now imperative and represents a pivotal concern for the continued advancement of renewable power.

Choosing appropriate energy storage technologies (ESTs) for varied operational contexts is fundamental to future energy planning, and contemporary mainstream ESTs generally fall into primary classes: mechanical energy storage, electrochemical energy storage (EES), chemical energy storage, thermal energy storage, and electrical energy storage [10, 11]. Distinct technical attributes govern each EST, leading to considerable variations in their ideal deployment settings, with certain technologies demanding highly specific installation environments [11, 13]. Financial expenditure is another paramount element determining the feasibility of an EST for broad commercialization. Any economic evaluation must encompass the technology's full life cycle, acknowledging that findings can vary drastically depending on the prevailing state of technological readiness, specific use cases, deployment logistics, geographical locations, and regulatory frameworks [10, 14]. By way of illustration, continuous innovations and favorable policies surrounding battery systems have spurred the accelerated deployment of EES facilities over the past decade, establishing them as essential ancillary systems for numerous decentralized solar and wind energy projects [15-17]. Furthermore, factoring in the lifecycle carbon footprint of an EST is crucial, as the existing industrial landscape cannot yet manufacture energy storage hardware and generate power relying exclusively on renewable inputs [18, 19]. Therefore, a holistic appraisal of the technical specifications, financial viability, and environmental sustainability of an EST across multiple frameworks is exceptionally valuable for validating its capacity for bulk energy storage [10, 11, 20].

Numerous prior investigations have analyzed the operational properties and techno-economic profiles of diverse ESTs, alongside the levelized cost of storage (LCOS) of EES across a range of applications like frequency control, voltage stabilization, and bulk storage [9, 11, 13-15, 21-24]. Rahman *et al*. [11] synthesized techno-economic and ecological evaluations spanning mechanical, electrochemical, chemical, and thermal technologies, identifying lifespan, operational efficiency, and cycle duration as the primary technical variables dictating financial and environmental outcomes. Bullich-Massagué *et al*. [13] explored optimal EST options for delivering diverse grid services within extensive solar installations, determining Li-ion batteries to be the superior alternative. Schmidt *et al*. [21] detailed the current LCOS across nine distinct ESTs while forecasting their developmental trajectories. Additionally, hydrogen energy storage (HES)—an emerging chemical storage approach offering substantial flexibility and broad applicability by utilizing electricity to synthesize hydrogen as a storable energy vector—has garnered significant attention across both academic and commercial sectors. Gu *et al.* [22] evaluated the LCOS and carbon emissions associated with extensive, long-range hydrogen transport by examining the triad of generation, distribution, and dispensing phases.

Nevertheless, their scope was restricted to three transport modalities: high-pressure trailers (20 MPa), liquid trailers, and chemical carriers (methanol) [22]. Following a comparable methodology, Paster *et al*. [23] quantified the LCOS and emission profiles for HES, expanding the analysis to include pipeline-based delivery systems. Despite these contributions, the majority of the literature has isolated single ESTs across varying frameworks, yielding scarce comparative analyses, and in-depth investigations that concurrently address both the financial expenditures and lifecycle carbon footprints of utility-scale ESTs remain rare. Certain evaluations have relied on proprietary commercial software [25, 26], resulting in opaque foundational cost data. Furthermore, the specific operational pathways of ESTs vary widely, and even for a solitary EST, disparate data sources can produce profound discrepancies in economic and environmental projections, severely complicating direct cross-technology comparisons drawn from independent studies [21].

In the present work, an initial comparative evaluation of ESTs viable for utility-scale deployment is executed based on their inherent technical properties. Subsequently, two promising variants, EES and HES, are isolated for more rigorous examination. A comprehensive lifecycle appraisal—encompassing the LCOS and carbon emissions of these two approaches across diverse contexts—is performed, with specific focus on the end-to-end implications of the HES configuration, using foundational data aggregated from diverse literature. Recognizing that substantial data volatility across sources introduces profound uncertainties, Monte Carlo simulations are applied to compute probability ranges for

© 2025 The Author(s). | Published by Institute of Smart Energy Systems Press

both financial expenditures and carbon footprints, thereby mitigating the influence of data unpredictability on the outcomes [27, 28]. Ultimately, ESTs applicable to massive-scale renewable integration are reviewed, and their prospective market competitiveness is gauged in light of the derived computational findings.

Materials and Methods

Selection of energy storage technology

This study begins by evaluating the technical parameters of various utility-scale ESTs to pinpoint those offering exceptional adaptability and extensive utility. Owing to constraints related to storage duration, energy limits, and stringent geographic prerequisites, certain ESTs prove inadequate for such scales. For example, electrical supercapacitors and mechanical flywheels frequently serve the purpose of recovering kinetic energy during automotive and railway deceleration, respectively [29, 30]. Although mechanical pumped hydroelectric storage represents a mature, economically viable solution that currently dominates over 90% of the global energy storage sector [31, 32], its implementation remains heavily constrained by topographical necessities, resulting in prolonged development cycles and restricted universal deployment [33]. In China, numerous territories boast abundant solar and wind potential [34]—specifically the eastern plains and northwestern sectors—but suffer from water scarcity and lack the proper terrain for pumped hydro facilities. Alternatively, thermal systems capture renewable power as heat, which can subsequently be utilized directly for warming or transformed back into electricity utilizing steam turbines within combined heat and power frameworks [35, 36].

A prime candidate for massive-scale deployment must possess universal applicability across varied environments, structural versatility, superior storage efficiency, and cost-effective long-range transport capabilities. Currently experiencing the most rapid global expansion in deployed capacity, EES adequately fulfills these baseline criteria. Furthermore, driven by relentless innovations in fuel cell engineering [2, 37-39], hydrogen energy storage (HES)—acting as a zero-emission energy vector [40-42] perfectly suited for both renewable integration and extended transmission—has captured significant academic and industrial focus.

Characterized by constructional adaptability and exceptional efficiency, EES frameworks typically capture volatile renewable power directly at the source when immediate grid integration is impossible. By discharging this stored power into the grid in response to demand fluctuations, these systems facilitate peak shaving and smooth the variability inherent in renewable generation **(Figure 1a)**. Prevalent battery architectures deployed in utility-scale grid operations primarily consist of lithium-ion (Li-ion), lead-acid (LA), sodium-sulfur (NaS), and vanadium redox flow (VRF) units [9, 11, 14]. Their contrasting operational traits are illustrated in **Figure 1b** [7, 11].

© 2025 The Author(s). | Published by Institute of Smart Energy Systems Press

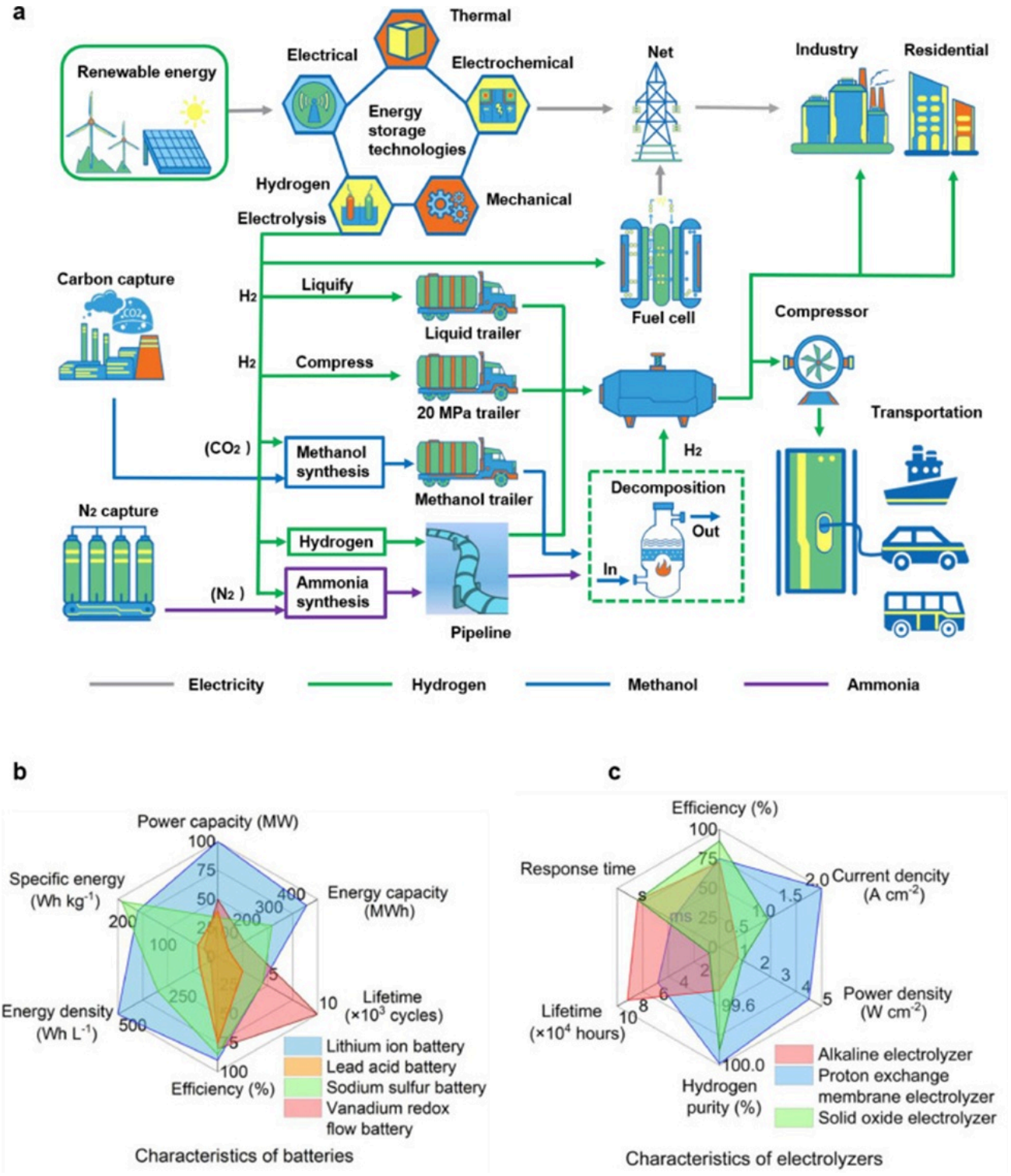


Figure 1. Roadmap and technical characteristics of promising large-scale renewable energy storage technologies. (a) A strategic blueprint for utility-scale energy storage within a prospective renewable-centric civilization. The primary objective of energy storage technologies (ESTs) is to mitigate the unpredictability of renewable yields, thereby circumventing grid integration hurdles and optimizing the equilibrium between power generation and consumption amidst escalating renewable penetration. The present analysis thoroughly investigates electrochemical energy storage (EES) and hydrogen energy storage (HES) as highly viable pathways for massive-scale operations. Within the EES paradigm, localized storage facilities capture intermittent renewable power before transmitting it through the grid. Conversely, the HES

© 2025 The Author(s). | Published by Institute of Smart Energy Systems Press

pathway incorporates multiple pivotal phases, notably hydrogen synthesis, transit from resource-dense zones to demand hubs, and subsequent refueling. (b) A technical comparison of distinct EES frameworks, encompassing lithium-ion (Li-ion), lead-acid (LA), sodium sulfur (NaS), and vanadium redox flow (VRF) battery systems [7, 11]. (c) An operational comparison of various electrolyzer technologies utilized for hydrogen generation, specifically an alkaline electrolyzer (AE), proton exchange membrane electrolyzer (PEME), and solid oxide electrolyzer (SOE) [43, 44].

In contrast to EES, hydrogen functions as an intrinsically stable and readily storable energy vector, enabling far more sophisticated and multifaceted application frameworks. This study holistically evaluates the fundamental components of HES, spanning hydrogen production (transforming power into hydrogen via water electrolysis), distribution (transit from generation nodes to final terminals), and dispensing (localized containment and end-user refueling) **(Figure 1a)**, with explicitly defined expenditures and emission profiles for each phase. Utilizing renewable electricity to drive water electrolysis is broadly recognized as the optimal strategy for synthesizing green hydrogen, effectively absorbing intermittent power while seamlessly integrating with massive-scale renewable architectures [40, 43, 45]. Contemporary commercial electrolysis hardware primarily comprises alkaline electrolyzers (AEs), proton exchange membrane electrolyzers (PEMEs), and solid oxide electrolyzers (SOEs) [43, 44, 46]. Their respective operational metrics are contrasted in **Figure 1c** [43, 44]. Frequently, high-demand energy hubs are situated at vast geographic distances from regions endowed with rich renewable assets. In China, for instance, a pronounced energy deficit exists along the southeastern seaboard—characterized by inadequate local generation or elevated tariffs.

In contrast, the northwestern territories hold massive renewable reserves separated by an expanse exceeding 2000 km [22]. Consequently, comprehensive distribution networks are obligatory for HES. For long-distance transport, these modalities broadly fall into two primary classifications: the direct delivery of hydrogen and the conveyance of hydrogen carriers. Direct hydrogen transport typically utilizes a 20 MPa trailer, liquid trailer, and hydrogen pipeline [22, 37]. Alternatively, conventional hydrogen vectors like methanol and ammonia are predominantly transported via trailers and pipeline networks, respectively [37, 47-49].

Economic model for EES

Typically, EES installations utilize a modular architecture, aggregating numerous battery modules in series and parallel arrangements to achieve the designated power and storage specifications. Accurately matching the facility's rated capacity to real-world operational demands is imperative. Factoring in both the overall system efficiency and the depth of discharge, the real capacity is derived using **Eq. 1.**

$$E_{\mathrm{EES}} = \frac{E_{\mathrm{R}}}{\eta_{\mathrm{b}} \times DOD} \quad (1)$$

Where EEES denotes the installed capacity (MWh) of the EES facility, ER signifies the rated capacity (MWh), represents the system efficiency (%) of the EES installation, and DOD indicates the depth of discharge (%).

Calculating the LCOS for an EES framework comprehensively accounts for expenditures related to capital investments, operations and maintenance, electricity inputs, necessary replacements, contingency reserves, and end-of-life recycling [7, 17, 21]. This metric can be computed via **Eq. 2.**

$$\mathrm{LCOS} = \frac{C_{\mathrm{cap}} + C_{\mathrm{OM}} + C_{E} + C_{\mathrm{rep}} + C_{\mathrm{con}} + C_{\mathrm{recycle}}}{P \times h_{\mathrm{d}} \times d} \left(\mathrm{US\$\,kWh^{-1}}\right) \quad (2)$$

Where Ccap defines the capital cost, COM designates the operations and maintenance cost, CE accounts for the electricity cost, Crep indicates the replacement cost, Ccon stands for the contingency cost, Crecycle reflects the end-of-

© 2025 The Author(s). | Published by Institute of Smart Energy Systems Press

life cost, P dictates the rated power, hd represents the operation hours per day, and d specifies the operation days per year.

The annualized capital expenditure is formulated utilizing **Eq. 3** [50, 51].

$$C_{cap} = C_{cap}^{total} \times \frac{i(1+i)^y}{(1+i)^y - 1} \quad (3)$$

Where refers to the total capital cost, while i and y correspond to the applicable discount rate and the expected service life, respectively.

Expenditures for operations and maintenance incorporate routine hardware servicing, the energy diverted to power the facility's internal systems, workforce remuneration, and similar overheads. By factoring in the projected annual fluctuation trajectory, the total operations and maintenance outlays for the present analysis are determined via **Eq. 4.**

$$C_{OM} = C_{OM}^{total} \times \left(\sum_{m=1}^{m=y} \frac{(1+V_{OM})^m}{(1+i)^m} \right) \times \frac{i(1+i)^y}{(1+i)^y - 1} \quad (4)$$

Where (US per year) signifies the total operations and maintenance cost per year, and VOM captures the annual factor change rate in operations and maintenance cost.

To accurately derive the ultimate terminal LCOS, expenditures for input electricity must be integrated into the financial model. This is quantified by **Eq. 5.**

$$C_E = B_{elec} \times d \times P \times \left(\frac{h_d}{\eta}\right) \times \left(\sum_{m=1}^{m=y} \frac{(1+V_{elec})^m}{(1+i)^m} \right) \times \frac{i(1+i)^y}{(1+i)^y - 1} \quad (5)$$

Where η represents the system efficiency, Belec denotes the electricity price (US kWh-1), and Velec defines the annual change rate of electricity prices, with specific baseline values.

Because individual battery units possess a finite number of charge and discharge cycles, the functional lifespan of an EES container inherently falls short of the facility's overarching structural design life, mandating periodic battery substitutions [7, 17, 50]. Nonetheless, it is crucial to emphasize that calculated replacement expenditures are strictly confined to the substitution of these energy storage containers [50]. Acknowledging the steady reduction in battery acquisition costs—spurred by rapid advancements across the energy storage sector—**Eq. 6** is applied to estimate the replacement outlay for an EES installation [17, 21, 22].

$$C_{rep} = B_{rep} \times E_{EES} \times N \times \left(\sum_{m=1}^{m=N} \frac{(1-V_{rep})^{m \times A}}{(1+i)^{m \times A}} \right) \times \frac{i(1+i)^y}{(1+i)^y - 1} \quad (6)$$

Where Crep designates the replacement cost (US per kWh per year), Brep corresponds to the replacement cost factor (US kWh^{-1}), N indicates the number of replacement times during a project's life cycle, Vrep tracks the annual change rate of the replacement cost, and A signifies the replacement years for the EES plants.

Recognizing that unpredictable complications are inevitable throughout the lifespan of any power storage facility, allocating a contingency cost (Ccon) is obligatory [11]. This reserve fund is established mathematically by **Eq. 7.**

© 2025 The Author(s). | Published by Institute of Smart Energy Systems Press

$$C_{con} = f_{con} \times C_{cap} \quad (7)$$

Where fcon serves as the coefficient of contingency cost; its exact value is extracted by multiplying the base capital investment by a specific multiplier.

Establishing comprehensive recycling protocols is a foundational pillar for any sustainable industrial sector. Preserving ecological integrity demands the systematic reclamation of viable hardware, alongside the specialized processing of components harboring hazardous materials like heavy metals and toxic elements [17, 50]. Nevertheless, owing to a pervasive absence of standardized recycling frameworks [7, 10]—combined with the fact that end-of-life processing represents merely a marginal fraction of the total LCOS [21, 52]—the present analysis excludes recycling expenditures from the economic model.

Economic model for HES

The levelized cost of storage (LCOS) for hydrogen, which accounts for synthesis, conveyance, and dispensing, is determined by **Eq. 8.**

$$\mathrm{LCOS} = \mathrm{C_{production}} + \mathrm{C_{delivery}} + \mathrm{C_{refueling}} \left(\mathrm{US\$\,kg^{-1}}\right) \quad (8)$$

In this expression, $C_{production}$, $C_{delivery}$, and $C_{refueling}$ denote the levelized costs associated with hydrogen generation, transportation, and refueling, respectively. The levelized expenditure for hydrogen generation mirrors the methodology applied to EES and is computed via **Eq. 9**.

$$C_{production} = \frac{C_{cap} + C_{OM} + C_E + C_{rep} + C_{con} + C_{recycle}}{m_{H_2}} \quad (9)$$

Here, signifies the mass flow of hydrogen synthesized annually (kg per year). The components C_{cap}, C_{OM}, C_E and C_{con} are determined in accordance with **Eqs. 3–5, and 7** previously established in this section. The replacement expenditure for hydrogen production infrastructure is derived using **Eq. 10.**

$$C_{rep} = D_{rep} \times P \times N \times \left(\sum_{m=1}^{m=N} \frac{(1 - V_{rep})^{m \times A}}{(1+i)^{m \times A}} \right) \times \frac{i(1+i)^y}{(1+i)^y - 1} \quad (10)$$

In this formula, D_{rep} (US\$ kW^{-1}) represents the replacement cost of the hydrogen generation facility. For hydrogen distribution via road transport, the levelized expenditure is derived from **Eq. 11**, noting that maintenance and fuel consumption outlays for compressors, liquid pumps, and tractors are subsumed within the operations and maintenance category.

$$C_{delivery} = \frac{C_{cap} + C_{OM}}{\frac{d}{T_{circle} \times m_{unit}}} \quad (11)$$

In this equation, m_{unit} denotes the mass capacity of the transport trailer, and T_{circle} represents the duration of a single delivery cycle. For delivery via pipeline, the levelized cost is determined by **Eq. 12** [37].

© 2025 The Author(s). | Published by Institute of Smart Energy Systems Press

$$C_{\text{delivery}} = \frac{\left(C_{\text{cap}}^{\text{total}} \times \frac{i(1+i)^t}{(1+i)^t - 1} \times t\right) + C_{\text{OM}} \times y}{y \times m_{\text{trans}}} \quad (12)$$

Here, t represents the capital payback period, y signifies the service life of the pipeline infrastructure, and m_{trans} indicates the annual mass flow of hydrogen. For a refueling installation, the expenditure is calculated by **Eq. 13.**

$$C_{\text{refueling}} = \frac{C_{\text{cap}} + C_{\text{OM}}}{m_{\text{scale}}} \quad (13)$$

In this expression, m_{scale} denotes the annual mass throughput of the refueling station, with corresponding economic parameters.

Carbon emissions

Emissions generated during battery manufacturing and operation constitute the overwhelming majority (over 90%) of the total carbon footprint for EES installations, whereas infrastructure assembly represents a minor fraction [53]. Consequently, to maintain simplicity, only battery-related emissions are evaluated. The carbon emission intensity (gCO2e kWh-1) is computed using **Eq. 14.**

$$E_{\text{CO}_2} = \frac{E_{\text{battery}}}{D_{\text{battery}} \times DOD \times \eta_b \times n_c} \times 10^6 \left(\text{gCO}_2\text{e kWh}^{-1}\right) \quad (14)$$

In this equation, E_{battery} refers to the carbon emissions attributable to battery fabrication (kg CO2e kg-1 battery), D_{battery} denotes the power density of the battery units (Wh kg-1), and n_c represents the cycle life of the batteries.

Regarding HES, the carbon footprint is evaluated across the entire lifecycle of production, transport, and dispensing. The synthesis phase for both HES and EES accounts for emissions arising from wind power generation, as well as the manufacturing and operation of electrolyzers. The distribution phase primarily encompasses emissions linked to pipeline fabrication and installation, while the dispensing phase includes those associated with hydrogen compression, containment, and refueling.

Data processing

While we aggregated data from recent scholarly publications, the reported values for individual parameters exhibited significant variability. Furthermore, the economic modeling proved exceptionally susceptible to numerical outliers. Relying on disparate data points would likely compromise the accuracy of our cost estimations. To mitigate the influence of these outliers, we utilized the Monte Carlo method to simulate extensive data samples derived from the original dataset. Before performing the Monte Carlo simulations, the interquartile range (IQR) of the raw data was established; the mean value of this IQR was then utilized as the representative figure for calculating the LCOS and carbon emissions of the ESTs. The results derived from these representative values and the Monte Carlo simulations are illustrated via bar charts and boxplots, respectively.

Results and Discussion

© 2025 The Author(s). | Published by Institute of Smart Energy Systems Press

Economy of electrochemical energy storage

The selection of battery technology profoundly influences the overall economic cost of EES installations. We evaluated the LCOS across four battery technologies, as illustrated in **Figure 2**. Given the variances in unit pricing, longevity, efficiency, and operational metrics, both the facility's service life and its energy storage capacity significantly affect the LCOS. Across the global landscape, the LCOS for most EES configurations—specifically Li-ion, NaS, and VRF batteries—declines as the project lifespan extends. Occasional increases in LCOS observed during specific years are primarily attributable to battery replacement expenditures necessitated by the finite cycle life of the hardware **(Figure 2a)**. Conversely, the LCOS for lead-acid (LA) batteries does not exhibit a substantial reduction over extended project durations; their optimal lifespan is limited to merely 10 years, which is notably shorter than the 20, 24, and 20-year optimal lifespans of the other three technologies. The relationship between energy capacity and LCOS was investigated by fixing the project lifespan at the optimal values for each technology **(Figure 2b)**. For all four battery types, the economies of scale regarding LCOS are monotonic; costs decrease as energy capacity increases, though the rate of reduction diminishes at higher capacities (exceeding 100 MWh). Of these, NaS batteries exhibit the most pronounced scale advantages, while Li-ion batteries demonstrate the lowest LCOS for capacities below 140 MWh. As capacity scales beyond this threshold, NaS batteries emerge as the most favorable option for minimizing LCOS.

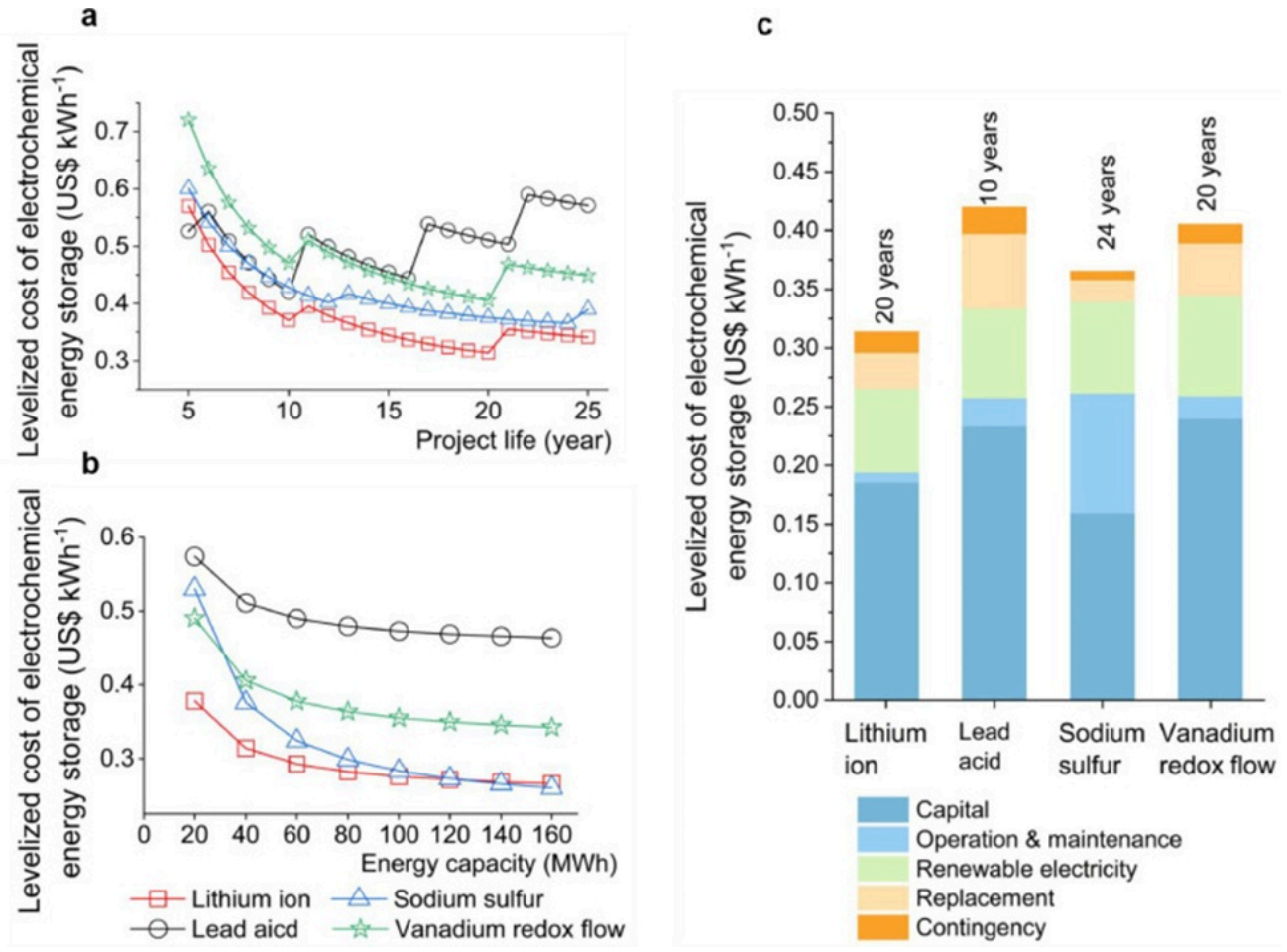


Figure 2. Comparative cost analysis of different electrochemical energy storage technologies. (a) Levelized costs of storage (LCOS) for different project lifetimes (5 to 25 years) for Li-ion, LA, NaS, and VRF batteries. (b) LCOS for different energy capacities (20 to 160 MWh) with the four batteries, and the power capacity is set to 20 MW. Among these batteries, the Li-ion battery has the lowest LCOS when the energy capacity is lower than 140 MWh. The NaS battery has a clear scale advantage over the other batteries; thus, the NaS battery would be the best choice for minimizing LCOS as energy capacity increases. (c) LCOS composition for the four batteries with energy and power capacities of 40 MWh and

© 2025 The Author(s). | Published by Institute of Smart Energy Systems Press

20 MW, respectively. The project lifetime is selected as the optimum solution for the four batteries, that is, 20, 10, 24, and 20 years. The LCOS detailed composition includes five categories: capital, operation & maintenance, renewable electricity, replacement, and contingency.

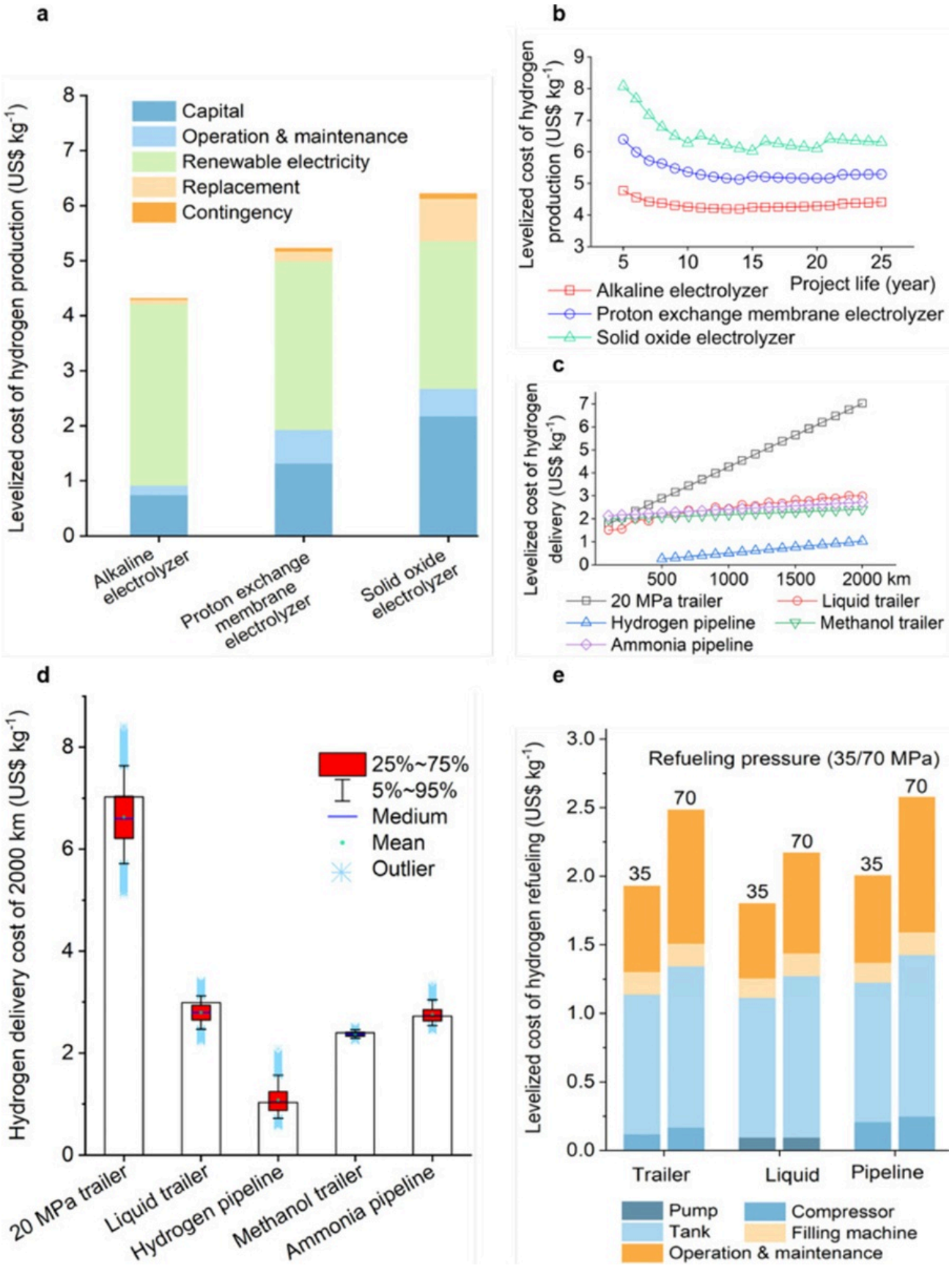
We further examined the specific cost structure of EES, which fundamentally consists of five segments: capital, operations and maintenance, renewable electricity (based on wind power costs), replacement, and contingency **(Figure 2c)**. Capital expenditure constitutes the most substantial portion of the total LCOS. For Li-ion units, capital costs account for 58.98% of the total, followed by renewable electricity costs at 22.74%. The cost structure for the remaining battery types follows a similar pattern, underscoring that curtailing capital expenditures—encompassing power conversion hardware, battery packs, and balance-of-plant infrastructure—is essential for reducing the LCOS of EES.

Within our defined scenarios (40 MWh energy capacity and 20 MW power capacity, utilizing optimal project lifespans for each), the Li-ion battery achieved the minimum LCOS of 0.314 US kWh-1. Furthermore, Li-ion batteries support significantly higher maximum rated power capacities compared to the alternatives **(Figure 1b)**, making them superior for applications requiring rapid power throughput. Due to their extended operational longevity, lower capital outlays, and scalability, NaS batteries also present a competitive profile, particularly for massive-scale storage deployments. Although the current LCOS for VRF batteries remains high, their inherent safety and the decoupling of power output from energy storage capacity offer operational advantages, ensuring their market viability contingent upon anticipated future cost reductions. The LA battery records the highest LCOS due to its brief operational life, notwithstanding the lower initial procurement costs. Nevertheless, LA batteries may remain economically viable for projects with a planned lifespan of less than five years **(Figure 1a).**

Economy of hydrogen energy storage

An evaluation and comparison of the levelized costs across all HES stages are provided **(Figure 3).** Regarding hydrogen synthesis, alkaline electrolysis (AE) yields the minimum levelized expense at 4.32 US kg-1 (per kg hydrogen). A granular breakdown of these expenditures indicates that powering the electrolyzers with renewable electricity constitutes the primary financial burden of hydrogen generation **(Figure 3a).** Specifically, when evaluating AE under the parameters of a 0.050 US kWh-1 electricity rate (based on wind power valuations [54]) and a 20-year operational span, renewable energy and capital outlays represent 76.23% and 17.14% of overall generation expenses, respectively. Furthermore, even for solid oxide electrolysis (SOE)—currently the least commercially mature option—capital investments comprise a mere 34.82% of total expenditures. Consequently, driving down renewable power prices remains the most critical mechanism for minimizing hydrogen generation expenses. Additionally, in stark contrast to electrical energy storage (EES), the financial outlay for producing hydrogen shows minimal sensitivity to the project's lifespan **(Figure 3b)**. For operational lifespans extending beyond 10 years, these cost variations become largely negligible. While AE stands as the most economical option today, proton exchange membrane electrolysis (PEME) demonstrates substantial promise to emerge as a dominant production technique. This potential is driven by its remarkable efficiency, impressive yield rates, superior gas purity, and robust compatibility with fluctuating renewable power inputs **(Figure 1c)** [8, 40, 55].

© 2025 The Author(s). | Published by Institute of Smart Energy Systems Press



© 2025 The Author(s). | Published by Institute of Smart Energy Systems Press

Figure 3. Comparative cost analysis for different hydrogen production, delivery and refueling methods for hydrogen energy storage. (a) Levelized costs and cost composition of hydrogen production via AE, PEME, and SOE. The price of renewable electricity is set to 0.05 US kWh-1. The rated power, load factor, working hours per day, and project lifetime are set to 50 MW, 46%, 24 h, and 20 years, respectively. (b) Effect of project lifetime on hydrogen production cost. (c) Effect of delivery distance on hydrogen delivery cost. (d) Levelized costs of hydrogen delivery via different delivery methods over 2000 km. The capacities of the 20 MPa trailer, liquid trailer, hydrogen pipeline, methanol trailer, and ammonia pipeline are 350 kg H2 per trailer, 4000 kg H2 per trailer, 131.6 tons H2 per day, 25 tons methanol per trailer, and 248.6 tons ammonia per day, respectively. The cost of synthesizing and cracking methanol and ammonia is included in the levelized cost of delivery. (e) Levelized costs of hydrogen refueling for 35 MPa and 70 MPa stations corresponding to different delivery methods, respectively. Different delivery methods cause refueling cost differences due to the use of different equipment and inlet pressures.

Expenses associated with transporting hydrogen form a vital component of the overall HES framework **(Figures 3c and 3d)**. Crucially, whenever hydrogen carriers like methanol or ammonia are utilized, the financial requirements for their synthesis and subsequent decomposition are integrated into this transportation phase. Assessing the various distribution networks reveals that pipeline infrastructure offers the greatest financial viability, predominantly for extended routes. Spanning a distance of 2000 km, pipeline transport achieves a remarkably low levelized cost of just 1.03 US kg-1, drastically undercutting alternative logistical approaches. By comparison, transporting liquid hydrogen incurs a levelized expense of 2.98 US kg-1, mirroring the financial requirements of methanol and ammonia distribution. Logistics distances inherently dictate these transportation expenditures; findings consistently highlight pipelines as the most cost-effective solution across all spans ranging between 500 and 2000 km (**Figure 3c**, establishing 500 km as the baseline pipeline distance). Conversely, for transit routes falling under 200 km, liquid and high-pressure trailers demonstrate superior economic feasibility compared to carrier-based ammonia and methanol logistics. Consequently, leveraging high-pressure trailers emerges as an optimal strategy for short-haul transport (under 200 km). This approach provides enhanced operational adaptability and minimized immediate expenditures, effectively circumventing both the massive initial capital required for pipeline networks and the specialized processing equipment demanded by chemical carriers.

This analysis models two distinct classifications of refueling infrastructure, specifically operating at pressures of 35 MPa and 70 MPa. Within these models, the static high-pressure gas reservoirs are designed to hold the equivalent of 2 days' worth of hydrogen demand. Additionally, the selected transportation modality can introduce variances in refueling expenditures; this phenomenon occurs because differing inlet pressures from various delivery mechanisms alter the energy demands—and thus the financial burden—of stationary compression. Despite these variations, the overall disparities in the levelized cost of hydrogen refueling across distinct transport logistics remain relatively constrained. For 35 MPa facilities, these values fluctuate between 1.80 and 2.01 US kg-1, whereas 70 MPa facilities see costs ranging from 2.17 to 2.58 US kg-1 **(Figure 3e)**. The bulk of refueling expenses is heavily concentrated in static hydrogen storage, with the stationary compression systems also representing a considerable financial commitment. Consequently, optimizing the station's internal hydrogen recirculation efficiency emerges as the primary mechanism for driving down expenses within the refueling stage.

Ultimately, the comprehensive LCOS for the entire HES—integrating generation, distribution, and refueling across multiple pathways—can be synthesized **(Figure 4a)**. These computations use a 35 MPa refueling baseline, combining the prior scenarios and datasets detailed in **Figures 3a, 3d, and 3e**. The most financially optimal HES framework combines AE generation, pipeline distribution, and matched refueling infrastructure. This specific trajectory achieves a minimal total LCOS of 7.52 US kg-1, with the generation, distribution, and refueling segments consuming 56.95%, 13.72%, and 29.33% of that total, respectively. In contrast, substituting pipeline transport with compressed gas, liquid formats, or chemical carriers (methanol and ammonia) drastically inflates the delivery segment's share to 52.93%, 33.20%, 26.98%, and 29.58% of the aggregate LCOS, respectively. Even when fully accounting for combined distribution and refueling expenditures, pipeline architectures maintain undisputed economic superiority for massive, long-haul energy transfer compared to competing delivery modes. Establishing pipeline logistics as the baseline, subsequent analysis evaluates how generation technologies influence the overarching HES economics. Depending on the specific electrolyzer deployed, the levelized expense of hydrogen synthesis constitutes between 56.95% and 66.11% of the complete LCOS—a bracket

© 2025 The Author(s). | Published by Institute of Smart Energy Systems Press

entirely beholden to renewable power pricing **(Figure 4b)**. Projections indicate that if renewable electricity tariffs fall to 0.02 US kWh-1, the aggregate LCOS and the specific proportional cost of AE generation would plummet to 5.58 US kg-1 and 42.02%, respectively. Building on these dynamics, an alternative paradigm is hypothesized, termed “on-site hydrogen production.” Under this model, hydrogen is generated immediately adjacent to demand centers utilizing locally sourced, albeit pricier, renewable power, thereby completely bypassing the need to import fuel from regions boasting abundant cheap renewables. The financial viability of this localized approach relies implicitly on the tariff delta between local green power and the electricity rates found in renewable-dense zones; specifically, the on-site model secures economic competitiveness provided the local renewable energy tariffs remain below 0.06 US kWh-1.

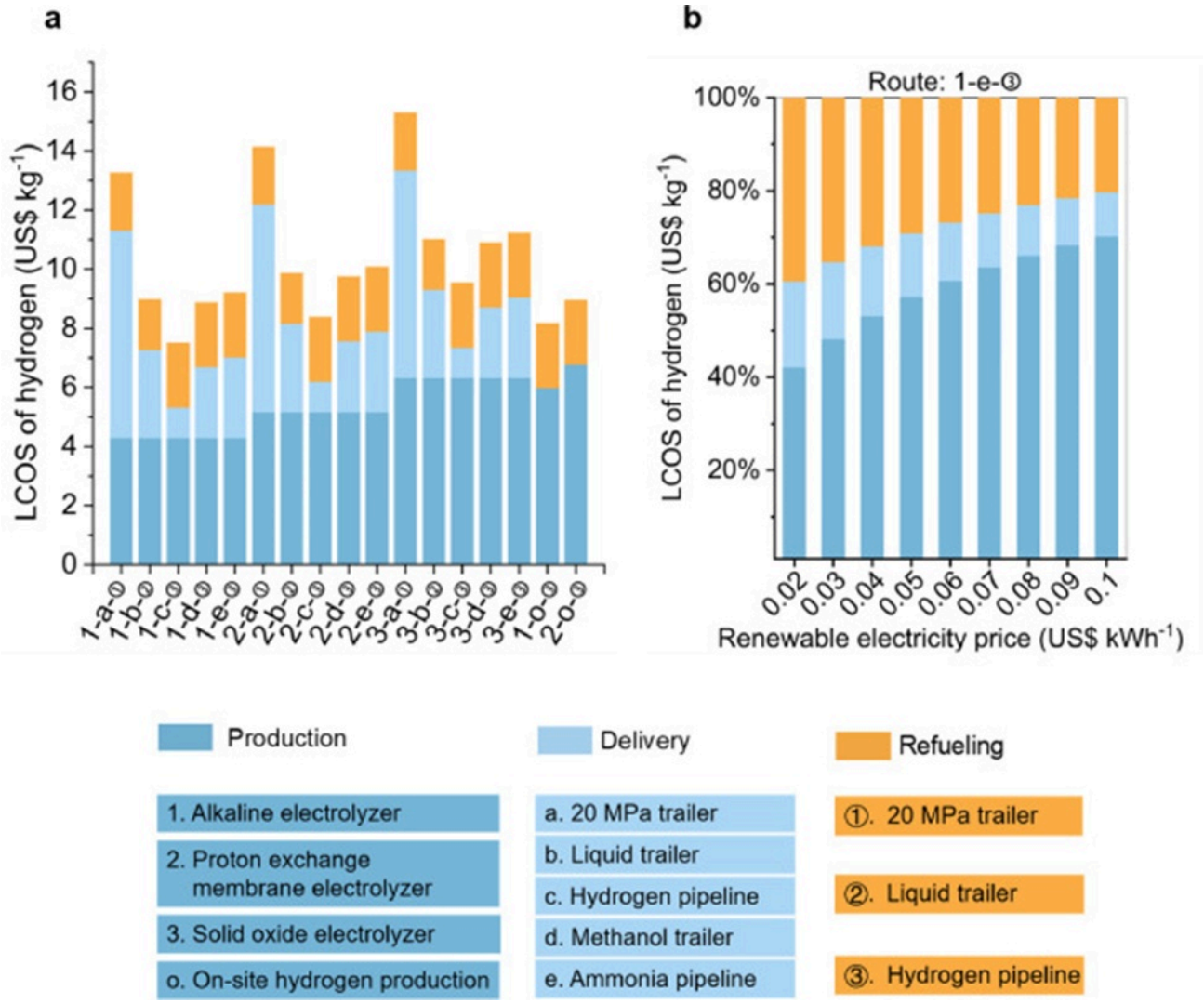


Figure 4. Cost analysis for hydrogen energy storage. (a) Overall LCOS for the HES evaluated across various configurations of hydrogen generation, transport, and station refueling. The distinct generation techniques are denoted by 1–3. The diverse transport strategies are indicated by a-e, while the refueling techniques, which are heavily reliant on the chosen transport mode, are marked as ①-③. Refueling approaches for chemical carriers mirror those utilized for pipelines, owing to the reduced inlet pressure characterizing the storage reservoirs. The generation pathway designated as “o” (on-site hydrogen production) indicates a scenario where hydrogen is synthesized locally within demand centers utilizing costlier renewable power, established at a rate of 0.075 US kWh-1. The specific HES configuration yielding the minimum LCOS integrates AE-based generation, pipeline distribution, and the associated refueling infrastructure. (b) A sensitivity assessment examining how fluctuations in renewable power pricing impact the financial breakdown of generation, transport, and refueling for the most economical pathway, 1-e-③, namely, generation via alkaline electrolyzer,

© 2025 The Author(s). | Published by Institute of Smart Energy Systems Press

pipeline distribution, and the matched refueling protocol. The modeled spectrum for renewable power tariffs spans from 0.02 to 0.1 US kWh-1, causing the cost share of AE-based generation to vary between 42.02% and 70.19% of the aggregate expenditures.

Comparison of electrochemical and hydrogen energy storage

Despite significant distinctions in their storage mechanisms and utilization profiles, evaluating the comparative costs of EES and HES is essential to assess the viability of these two energy storage technologies (ESTs), which serve comparable roles in accommodating large-scale renewable power generation. To establish an equivalent basis for this comparison, the specific cost (US kWh-1) and carbon footprint (gCO2e kWh-1) are computed for HES configurations utilizing various generation techniques (three distinct electrolyzers) and EES systems employing different battery types. For these calculations, hydrogen is quantified based on its calorific value of 33.33 kWh per kg H2 **(Figure 5a).** Within the HES framework, pipeline transport is selected for hydrogen distribution, as it offers the minimum levelized cost among transport alternatives. This assumes a 2000 km distribution span, modeling long-distance, cross-regional energy transfer typical of China **(Figure 5a)**. Findings indicate that the minimum LCOS achieved by HES stands at 0.227 US kWh-1 (utilizing AE generation). In contrast, the EES equivalent is 0.314 US kWh-1 (utilizing Li-ion batteries). Consequently, the optimal LCOS for HES equates to 72.20% of the optimal EES cost. It must be acknowledged that there remains a substantial disparity in the energy quality between hydrogen and direct electricity. To contextualize this, a transportation-based scenario is evaluated. A standard light-duty fuel cell passenger car utilizes 0.91 kg per 100 km [23], translating to a hydrogen fuel expenditure of 6.88 US per 100 km. This operational expense closely rivals the fueling costs of conventional diesel or gasoline internal combustion vehicles.

© 2025 The Author(s). | Published by Institute of Smart Energy Systems Press

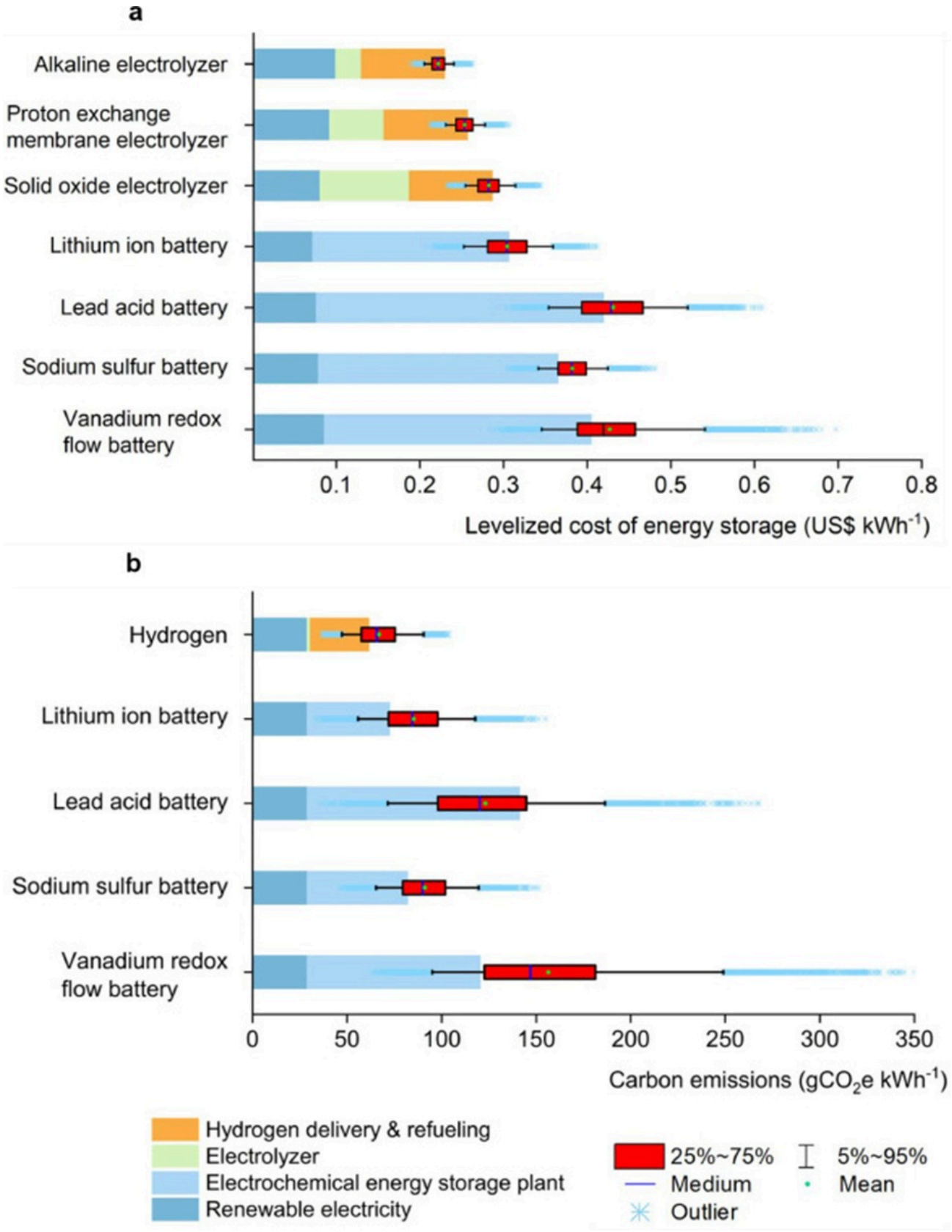


Figure 5. Comparative cost and carbon emissions analyses of hydrogen energy storage and electrochemical energy storage and their uncertainty ranges. a, Breakdown of LCOS, cost components, and uncertainty intervals for HES across

© 2025 The Author(s). | Published by Institute of Smart Energy Systems Press

various generation techniques, alongside corresponding metrics for four EES battery types. In the HES model, transport occurs via pipeline, with generation expenses split between renewable power and the electrolyzer infrastructure. For the EES model, expenses are separated into renewable electricity and EES facilities (encompassing construction, operational, and maintenance costs). b, Comprehensive breakdown of carbon footprints and associated uncertainty margins for HES and the four EES battery configurations. Given that electrolyzer-induced carbon emissions represent a marginal fraction of the aggregate footprint (roughly 4%) [56], variations in emissions among the different electrolyzer technologies are not considered herein. The overall carbon footprint for HES is calculated at 61.63 gCO2e kWh-1, with renewable energy (based on wind power metrics) responsible for 46.56% of these total emissions. Conversely, in EES frameworks, a substantial majority of carbon emissions stem from battery fabrication and system operation. Among EES options, Li-ion batteries exhibit the minimal carbon footprint at 72.76 gCO2e kWh-1, wherein operational processes and battery manufacturing constitute 60.56% of the overall emissions.

A deeper investigation into the relative carbon footprints of EES and HES is also conducted **(Figure 5b)**. Because the varying electrolyzer types contribute only marginally to overall carbon output (roughly 4%) [56], disparities across these specific technologies are omitted from the HES assessment. The total carbon footprint of the HES pathway measures 61.63 gCO2e kWh-1. Of this total, renewable energy generation is responsible for 46.56%, whereas the combination of electrolyzer fabrication, operational activities, distribution, and refueling accounts for the remaining 53.44%. In contrast, EES systems demonstrate heavy carbon expenditures concentrated in the manufacturing and operation phases. The Li-ion chemistry offers the most environmentally favorable EES profile, registering 72.76 gCO2e kWh-1, with plant construction and ongoing operations contributing 60.56% of these aggregate emissions. Sodium-sulfur (NaS) batteries similarly exhibit competitive capabilities in mitigating carbon output. When evaluating HES against EES, hydrogen-based storage has a clear environmental advantage in carbon emissions, primarily because electrolyzer fabrication, along with hydrogen logistics and storage, produces fewer emissions than the intensive manufacturing required for chemical batteries.

Uncertainty analysis

A Monte Carlo simulation is deployed to investigate the uncertainty margins surrounding the computed LCOS and carbon emission values. LCOS metrics for EES display substantial variability. Specifically, the 5%−95% uncertainty intervals for Li-ion, LA, NaS, and VRF systems span 82.88%−117.99%, 82.04% to 120.57%, 89.31% to 111.11%, and 80.94% to 126.62% relative to their corresponding mean figures, respectively **(Figure 5a)**. Furthermore, evaluating the variation coefficient of the LCOS provides insight into the dispersion level of these findings. The analysis reveals severe financial uncertainty within EES due to broad fluctuations across input variables. The resulting LCOS distribution for electrochemical storage is positively skewed, indicating a higher concentration of cost probabilities on the lower (left) end with an extended tail toward the higher (right) side. Statistical outliers are predominantly located at the upper extreme of the cost spectrum, while the mean expenditure gravitates toward the lower end. This pattern suggests that overall pricing tends to remain lower; notably, the deterministic calculations performed herein closely align with the statistical averages derived from the uncertainty modeling, confirming that the chosen input parameters are logical and representative of most standard scenarios. The broad uncertainty intervals and elevated coefficients of variation suggest an absence of a singular, dominant battery technology. Despite its maturity, the lead-acid (LA) battery exhibits the broadest span of uncertainty. This is hypothesized to result from a highly fragmented manufacturing sector comprising numerous producers, which introduces vast disparities in product quality and market pricing. Conversely, the production of NaS batteries is heavily consolidated among a select group of Japanese corporations, ensuring highly standardized pricing and, consequently, minimal financial uncertainty [57].

Regarding the HES pathways, the 5%−95% LCOS uncertainty bounds utilizing AE, PEME, and SOEC generation correspond to 92.31%−108.61%, 91.01%−109.80%, and 89.87%−111.42% of their specific average values, respectively **(Figure 5a)**. Across these distinct hydrogen generation techniques, the levelized cost variation coefficient remains under 8%, a relatively tight margin that reinforces the reliability of the findings. These outcomes demonstrate that the choice of hydrogen generation technology does not critically alter the overarching financial uncertainty of the HES system. The levelized expenses corresponding to diverse hydrogen transportation protocols are mapped out in **Figure 3d**. While

© 2025 The Author(s). | Published by Institute of Smart Energy Systems Press

pipeline distribution maintains a decisive financial advantage over competing methods, it simultaneously suffers from profound uncertainty, exhibiting a variation coefficient peaking at 24.12%. This elevated variance is attributed to the nascent developmental stage of dedicated hydrogen pipelines and a prevailing absence of widespread commercial implementations. When evaluating the aggregate expenditure of HES frameworks, the observed uncertainty margins remain fundamentally narrower than those affecting EES **(Figure 5a)**. Like EES, the levelized cost probability distribution for hydrogen storage remains positively skewed. Moreover, as the baseline cost of an HES configuration escalates, its corresponding band of uncertainty progressively widens.

Environmental uncertainty margins closely parallel those observed in the financial analysis. The NaS chemistry demonstrates the most constrained uncertainty regarding carbon output. In contrast, LA displays the most extensive variability **(Figure 5b)**. The probability density for carbon emissions is more concentrated on the lower (left) axis, similarly reflecting a positively skewed distribution. This variability is directly correlated with industrial fabrication dynamics; a larger pool of market manufacturers inherently drives higher levels of emission uncertainty. The carbon footprint uncertainty intervals for Li-ion, LA, NaS, and VRF battery systems span 65.4%−138.2%, 58.1% to 151.0%, 71.7% to 131.4%, and 60.8% to 159.3% of their respective mean projections **(Figure 5b)**. Conversely, the environmental uncertainty bounds for HES range between 85.8% and 113.2% of its mean value, a span significantly tighter than any EES counterpart. Consequently, when deployed for massive, prolonged energy buffering, HES emerges as a superior, eco-friendly alternative to chemical batteries, poised to play a crucial part in broader decarbonization efforts.

Conclusion

Through initial technical evaluations, this investigation identifies and selects two highly promising energy storage technologies: EES and HES. A rigorous, lifecycle-spanning implementation model is constructed for both storage paradigms to assess their respective financial demands and carbon outputs. Foundational data supporting this modeling were systematically aggregated from diverse literature sources. At the same time, a subsequent Monte Carlo simulation was executed to mitigate the inherent unreliability caused by discrepancies across these disparate data pools. Findings confirm that the predominant share of both financial outlays and environmental degradation associated with EES stems directly from capital investments—specifically, the industrial fabrication of the batteries and the construction of the facility infrastructure spanning all four predominant chemistries (Li-ion, LA, NaS, and VRF). Across most evaluated conditions, Li-ion setups secure both the lowest carbon footprint and the most economical LCOS among the chemical battery options, yielding a calculated LCOS of 0.314 US kWh-1 within a closely detailed operational framework. However, probabilistic modeling reveals wide uncertainty margins and steep variation coefficients for the LCOS and environmental impact of all four battery variants, indicating that no single chemistry possesses absolute technological or economic dominance. For the HES architecture, the financial viability of hydrogen synthesis is shown to be acutely dependent on prevailing renewable power tariffs.

Furthermore, for distribution routes spanning 500-2000 km (assuming a 500 km baseline for pipeline viability), transporting hydrogen via dedicated pipelines yields the lowest levelized expenditure when compared with liquid trailers, compressed gas haulage, or chemical carriers like ammonia and methanol. While varying transportation mechanisms inherently influence final refueling expenses, these station-side costs are most strongly dictated by the scale of the localized stationary storage systems. The most financially advantageous HES trajectory combines AE-driven generation, pipeline-based distribution, and compatible refueling infrastructure. Within a specific operational scenario, this optimal pathway achieves an LCOS of 7.52 US kg-1, with the generation, transport, and station components claiming 56.95%, 13.72%, and 29.33% of the aggregate expense, respectively. By converting hydrogen metrics into equivalent calorific values, a direct techno-economic and environmental comparison between EES and HES is facilitated. Under optimal configurations, HES reaches a minimum LCOS of 0.227 US kWh-1 alongside a carbon footprint of 61.63 gCO2e kWh-1, whereas the optimal EES benchmarks settle at 0.314 US kWh-1 and 72.76 gCO2e kWh-1, respectively. Despite intrinsic differences in the functional energy quality between direct electricity and chemical hydrogen, procuring hydrogen at a rate of 7.52 US kg-1 proves profoundly competitive and economically justifiable for deployment within the transportation

© 2025 The Author(s). | Published by Institute of Smart Energy Systems Press

sector. Looking toward future optimization, this research posits that driving down renewable power tariffs, boosting the conversion efficiencies of water electrolyzers, deploying extensive pipeline networks, and minimizing station-level storage durations via artificial intelligence planning represent vital mechanisms for continuously slashing both the financial and environmental costs of HES. Concurrently, reducing the initial capital expenditures and carbon emissions associated with manufacturing remains the critical developmental imperative for advancing EES.

Abbreviations

EST = Energy storage technology

EES = Electrochemical energy storage

HES = Hydrogen energy storage

LCOS = Levelized cost of storage

AE = Alkaline electrolyzer

PEME = Proton exchange membrane electrolyzer

SOE = Solid oxide electrolyzer

Li-ion = Lithium-ion

LA = Lead acid

NaS = Sodium sulfur

VRF = Vanadium redox flow

Acknowledgements

None

Conflict of interest

None

Financial support

This research is supported by the National Natural Science Foundation of China (No. 51921004). B. Wang thanks the funding support from the Hong Kong Scholars Program (No. XJ2021033).

Ethics statement

None

Received: 21 Aug 2023 Revised: 27 Oct 2023 Accepted: 13 Nov 2023
Published online: 15 June 2025

© 2025 The Author(s). | Published by Institute of Smart Energy Systems Press

Rights and permissions

Open Access The author(s) retain copyright. This article is licensed under the Creative Commons Attribution-NonCommercial-ShareAlike 4.0 International License. It may be shared and adapted for non-commercial purposes with appropriate attribution, an indication of changes, and distribution of adaptations under the same license. Third-party material may be subject to separate terms identified in its credit line. View the license at https://creativecommons.org/licenses/by-nc-sa/4.0/.

References

1. Jeff T. Nations must triple efforts to curb greenhouse-gas emissions. Nature. 2018 Nov 27;563(7733):591. https://doi.org/10.1038/d41586-018-07566-9.

2. Jiao K, Xuan J, Du Q, Bao Z, Xie B, Wang B, et al. Designing the next generation of proton-exchange membrane fuel cells. Nature. 2021;595(7867):361-9.

3. Meinshausen M, Jeffery L, Guetschow J, Robiou Du Pont Y, Rogelj J, Schaeffer M, et al. National post-2020 greenhouse gas targets and diversity-aware leadership. Nat Clim Change. 2015;5(12):1098-106.

4. Camarasa C, Mata É, Navarro JPJ, Reyna J, Bezerra P, Angelkorte GB, et al. A global comparison of building decarbonization scenarios by 2050 towards 1.5–2 °C targets. Nat Commun. 2022;13(1):3077.

5. Jewell J, McCollum D, Emmerling J, Bertram C, Gernaat DEHJ, Krey V, et al. Limited emission reductions from fuel subsidy removal except in energy-exporting regions. Nature. 2018;554(7691):229-33.

6. Wang T, Jiang Z, Zhao B, Gu Y, Liou K, Kalandiyur N, et al. Health co-benefits of achieving sustainable net-zero greenhouse gas emissions in California. Nat Sustain. 2020;3(8):597-605.

7. Mostafa MH, Abdel Aleem SHE, Ali SG, Ali ZM, Abdelaziz AY. Techno-economic assessment of energy storage systems using annualized life cycle cost of storage (LCCOS) and levelized cost of energy (LCOE) metrics. J Energy Storage. 2020;29:101345.

8. Lehner M, Tichler R, Steinmüller H, Koppe M. Power-to-Gas: technology and business models. Cham: Springer International Publishing; 2014. https://doi.org/10.1007/978-3-319-03995-4.

9. Koohi-Fayegh S, Rosen MA. A review of energy storage types, applications and recent developments. J Energy Storage. 2020;27:101047.

10. Zakeri B, Syri S. Electrical energy storage systems: a comparative life cycle cost analysis. Renew Sustain Energy Rev. 2015;42:569-96.

11. Rahman MM, Oni AO, Gemechu E, Kumar A. Assessment of energy storage technologies: a review. Energy Convers Manage. 2020;223:113295.

12. Research for greener batteries. Nat Sustain. 2021;4:373.

13. Bullich-Massagué E, Cifuentes-García F, Glenny-Crende I, Cheah-Mañé M, Aragüés-Peñalba M, Díaz-González F, et al. A review of energy storage technologies for large scale photovoltaic power plants. Appl Energy. 2020;274:115213.

14. Poonpun P, Jewell WT. Analysis of the cost per kilowatt hour to store electricity. IEEE Trans Energy Convers. 2008;23(2):529-34.

15. Boretti A. Integration of solar thermal and photovoltaic, wind, and battery energy storage through AI in NEOM city. Energy and AI. 2021;3:100038.

© 2025 The Author(s). | Published by Institute of Smart Energy Systems Press

16. Ibrahim H, Ilinca A, Perron J. Energy storage systems—Characteristics and comparisons. Renew Sustain Energy Rev. 2008;12(5):1221-50.

17. Schmidt O, Hawkes A, Gambhir A, Staffell I. The future cost of electrical energy storage based on experience rates. Nat Energy. 2017;2(8):1-8.

18. Rogelj J, Schaeffer M, Meinshausen M, Knutti R, Alcamo J, Riahi K, et al. Zero emission targets as long-term global goals for climate protection. Environ Res Lett. 2015;10(10):105007.

19. Wei W, Li J, Chen B, Wang M, Zhang P, Guan D, et al. Embodied greenhouse gas emissions from building China's large-scale power transmission infrastructure. Nat Sustain. 2021;4(8):739-47.

20. Olabi AG, Onumaegbu C, Wilberforce T, Ramadan M, Abdelkareem MA, Al Alami AH. Critical review of energy storage systems. Energy. 2021;214:118987.

21. Schmidt O, Melchior S, Hawkes A, Staffell I. Projecting the future levelized cost of electricity storage technologies. Joule. 2019;3(1):81-100.

22. Gu Y, Chen Q, Xue J, Tang Z, Sun Y, Wu Q. Comparative techno-economic study of solar energy integrated hydrogen supply pathways for hydrogen refueling stations in China. Energy Convers Manag. 2020;223:113240.

23. Paster MD, Ahluwalia RK, Berry G, Elgowainy A, Lasher S, McKenney K, et al. Hydrogen storage technology options for fuel cell vehicles: well-to-wheel costs, energy efficiencies, and greenhouse gas emissions. Int J Hydrog Energy. 2011;36(22):14534-51.

24. Battke B, Schmidt TS, Grosspietsch D, Hoffmann VH. A review and probabilistic model of lifecycle costs of stationary batteries in multiple applications. Renew Sustain Energy Rev. 2013;25:240-50.

25. Santoyo-Castelazo E, Gujba H, Azapagic A. Life cycle assessment of electricity generation in Mexico. Energy. 2011;36(3):1488-99.

26. Nugent D, Sovacool BK. Assessing the lifecycle greenhouse gas emissions from solar PV and wind energy: a critical meta-survey. Energy Policy. 2014;65:229-44.

27. Tian X, Stranks SD, You F. Life cycle assessment of recycling strategies for perovskite photovoltaic modules. Nat Sustain. 2021;4(9):821-9.

28. Madhu K, Pauliuk S, Dhathri S, Creutzig F. Understanding environmental trade-offs and resource demand of direct air capture technologies through comparative life-cycle assessment. Nat Energy. 2021;6(11):1035-44.

29. Olabi AG, Abbas Q, Al Makky A, Abdelkareem MA. Supercapacitors as next generation energy storage devices: properties and applications. Energy. 2022;248:123617.

30. Li X, Palazzolo A. A review of flywheel energy storage systems: state of the art and opportunities. J Energy Storage. 2022;46:103576.

31. Luo X, Wang J, Dooner M, Clarke J. Overview of current development in electrical energy storage technologies and the application potential in power system operation. Appl Energy. 2015;137:511-36.

32. Barbaros E, Aydin I, Celebioglu K. Feasibility of pumped storage hydropower with existing pricing policy in Turkey. Renew Sustain Energy Rev. 2021;136:110449.

33. Hunt JD, Zakeri B, Lopes R, Barbosa PSF, Nascimento A, Castro NJD, et al. Existing and new arrangements of pumped-hydro storage plants. Renew Sustain Energy Rev. 2020;129:109914.

© 2025 The Author(s). | Published by Institute of Smart Energy Systems Press

34. State Grid of China. The dispatch of clean energy, http://www.sgcc.com.cn/ywlm/index.shtml; 2022 [accessed 24 June 2022].

35. Gil A, Medrano M, Martorell I, Lázaro A, Dolado P, Zalba B, et al. State of the art on high temperature thermal energy storage for power generation. Part 1—Concepts, materials and modellization. Renew Sustain Energy Rev. 2010;14(1):31-55.

36. Liu HB, Zhao CY. Effect of radial porosity oscillation on the thermal performance of packed bed latent heat storage. Engineering. 2021;7(4):515-25.

37. Miao B, Giordano L, Chan SH. Long-distance renewable hydrogen transmission via cables and pipelines. Int J Hydrog Energy. 2021;46(36):18699-718.

38. Jiao K, Wang B, Du Q, Wang Y, Zhang G, Yang Z, et al. Water and thermal management of proton exchange membrane fuel cells. Amsterdam: Elsevier; 2021. https://doi.org/10.1016/C2020-0-04110-1.

39. Wang J, Wang H, Fan Y. Techno-economic challenges of fuel cell commercialization. Engineering. 2018;4(3):352-60.

40. Fang R. Life cycle cost assessment of wind power–hydrogen coupled integrated energy system. Int J Hydrog Energy. 2019;44(56):29399-408.

41. Tong L, Bénard P, Zong Y, Chahine R, Liu K, Xiao J. Artificial neural network based optimization of a six-step two-bed pressure swing adsorption system for hydrogen purification. Energy and AI. 2021;5:100075.

42. Zhang X. The development trend of and suggestions for China's hydrogen energy industry. Engineering. 2021;7(6):719-21.

43. Ochoa Robles J, De-León Almaraz S, Azzaro-Pantel C. Hydrogen supply chains. New York: Academic Press; 2018. https://doi.org/10.1016/B978-0-12-811197-0.00002-6.

44. Shiva Kumar S, Himabindu V. Hydrogen production by PEM water electrolysis – A review. Mater Sci Technol. 2019;2(3):442-54.

45. Sun H, Ebadi AG, Toughani M, Nowdeh SA, Naderipour A, Abdullah A. Designing framework of hybrid photovoltaic-biowaste energy system with hydrogen storage considering economic and technical indices using whale optimization algorithm. Energy. 2022;238:121555.

46. Sebbahi S, Nabil N, Alaoui-Belghiti A, Laasri S, Rachidi S, Hajjaji A. Assessment of the three most developed water electrolysis technologies: alkaline water electrolysis, proton exchange membrane and solid-oxide electrolysis. Mater Today Proc. 2022;66:140-5.

47. Bicer Y, Dincer I, Zamfirescu C, Vezina G, Raso F. Comparative life cycle assessment of various ammonia production methods. J Clean Prod. 2016;135:1379-95.

48. Makhloufi C, Kezibri N. Large-scale decomposition of green ammonia for pure hydrogen production. Int J Hydrog Energy. 2021;46(70):34777-87.

49. McKinlay CJ, Turnock SR, Hudson DA. Route to zero emission shipping: hydrogen, ammonia or methanol? Int J Hydrog Energy. 2021;46(55):28282-97.

50. Kebede AA, Coosemans T, Messagie M, Jemal T, Behabtu HA, Van Mierlo J, et al. Techno-economic analysis of lithium-ion and lead-acid batteries in stationary energy storage application. J Energy Storage. 2021;40:102748.

51. Kazi M, Eljack F, El-Halwagi MM, Haouari M. Green hydrogen for industrial sector decarbonization: costs and impacts on hydrogen economy in Qatar. Comput Chem Eng. 2021;145:107144.

© 2025 The Author(s). | Published by Institute of Smart Energy Systems Press

52. Arshad F, Lin J, Manurkar N, Fan E, Ahmad A, Tariq M, et al. Life cycle assessment of lithium-ion batteries: a critical review. Resour Conserv Recycl. 2022;180:106164.

53. Dehghani-Sanij AR, Tharumalingam E, Dusseault MB, Fraser R. Study of energy storage systems and environmental challenges of batteries. Renew Sustain Energy Rev. 2019;104:192-208.

54. Adnan M, Ahmad J, Ali SF, Imran M. A techno-economic analysis for power generation through wind energy: a case study of Pakistan. Energy Rep. 2021;7:1424-43.

55. Hu G, Chen C, Lu HT, Wu Y, Liu C, Tao L, et al. A review of technical advances, barriers, and solutions in the power to hydrogen (P2H) roadmap. Engineering. 2020;6(12):1364-80.

56. Cetinkaya E, Dincer I, Naterer GF. Life cycle assessment of various hydrogen production methods. Int J Hydrog Energy. 2012;37(3):2071-80.

57. Skyllas-Kazacos M. Stand-alone and hybrid wind energy systems. Cambridge: Woodhead Publishing; 2010. https://doi.org/10.1533/9781845699628.2.323.

© 2025 The Author(s). | Published by Institute of Smart Energy Systems Press